José D. Ruiz-Álvarez

28 August 2014

Chapter 1

The CMS experiment at LHC

The CMS experiment is one of the biggest particle physics experiments on the world. It is located at the ring of the LHC that is the main experience managed by CERN, the European Organization for Nuclear Research or Centre Européenne pour la Recherche Nucléaire by its name on french. This center constitutes the biggest center for research on particle physics all over the world. All along its 60 years of existence, from 1954, 21 member states have been joining it, but an overall of 113 countries participate in different ways on this center.

On the present chapter we discuss in detail different aspects of the LHC accelerator and the CMS experiment. In particular we make some emphasis in the CMS sub-detectors related to jets, objects that play the main role on the search that is the main subject of the present work. We also discuss the present state of both machines, their achievements and the challenges that were came through. Finally, also the expectations and goals for the upcoming run II are mentioned.

1.1 The Large Hadron Collider

The Large Hadron Collider, or LHC [1], is a machine that accelerates and collides protons and heavy ions. This machine is the biggest particle collider nowadays with a circumference of 27 km. It also achieves the greatest energy by a collider up to present, planned to be 14 TeV at the center of mass of the collision. On the first run of the machine only 8 TeV were achieved, and next run is planned to start with 13 TeV. It's located in French-Swiss border near to Geneva. The tunnel for the machine was carved around 100 m under the ground, 45 m under the Jura mountains and 170 m under the Léman lake with an inclination of around 1.4%, sloping down towards the lake . This machine has used as much as possible old LEP buildings and sites, that was an electron-positron collider built between 1984 and 1989.

The protons and heavy ions accelerated by the machine are collided in different points where dedicated experiments are located to detect and study the product from the collisions. The four main experiments located on the LHC ring are CMS [2, 3], ATLAS [4], LHCb [5] and ALICE [6]. The first two are experiments of generic purpose

where searches for new physics and also precision measurements are performed. LHCb is dedicated to the physics of the b-quark, and ALICE focuses on the study of the quark-gluon plasma produced from heavy ions collisions. However one of the principal objectives of the construction of the LHC was the discovery of the Higgs boson, generic searches on new physics have been conducted from the very beginning of the first data taking on 2009. Moreover, after the Higgs discovery on 2012 there is a growing effort on the searches for new physics and precision measurement on the properties of the Higgs.

The LHC is a complex machine composed of several parts. The two principal parts are the injector chain and the main ring. A diagram of the whole CERN complex can be seen in figure 1.1. The injector chain has different stages that pre-accelerate protons and heavy ions to be injected into the main ring of LHC. In the main ring the protons and heavy ions are fully accelerated and collided in four different points over the ring.

1.1.1 Injector chain

The injector chain begins with the proton source. Protons are extracted via ionization of Hydrogen gas in the Duoplasmatron Proton Ion Source. Such extraction is pulsed, what makes up the first bunch structure. The extracted protons are then accelerated to 50 MeV in the linear accelerator, Linac2, that dates from 1978. After this first stage several steps are followed:

1. Linac2 injects proton bunches in the Proton Synchrotron Booster (PSB) where are accelerated to 1.4 GeV.

2. From PSB, the protons are delivered to the Proton Synchrotron (PS) where they reach an energy of 25 GeV. In the PS the bunches are also split from 6 initial bunches to 72 spaced by 25 ns.

3. Finally, the pre-acceleration chain is finished by the SPS, Super Proton Synchrotron. There the bunches are accelerated up to 450 GeV right before being inserted to the main LHC ring.

The whole pre-acceleration chain has been optimized to obtain the best possible performance on the final acceleration in the LHC main ring. All parameters are carefully controlled, for example the number of bunches, the separation between bunches, the separation between trains of bunches or the injection energy to each subsystem. It's also remarkable to notice the level of control achieved in the bunches manipulation, from old subsystems as the PS from 1959 or the newest, the SPS that dates from 1976.

Some recent plans for future accelerator have been theorized using the LHC main ring as injector for a bigger accelerator, for example the so called Very Large Hadron Collider or VLHC.

1.1.2 Main ring

The main ring is composed of two rings that accelerate the proton bunches in opposite directions, clock-wise and counter clock-wise. An schematic view of the design of the

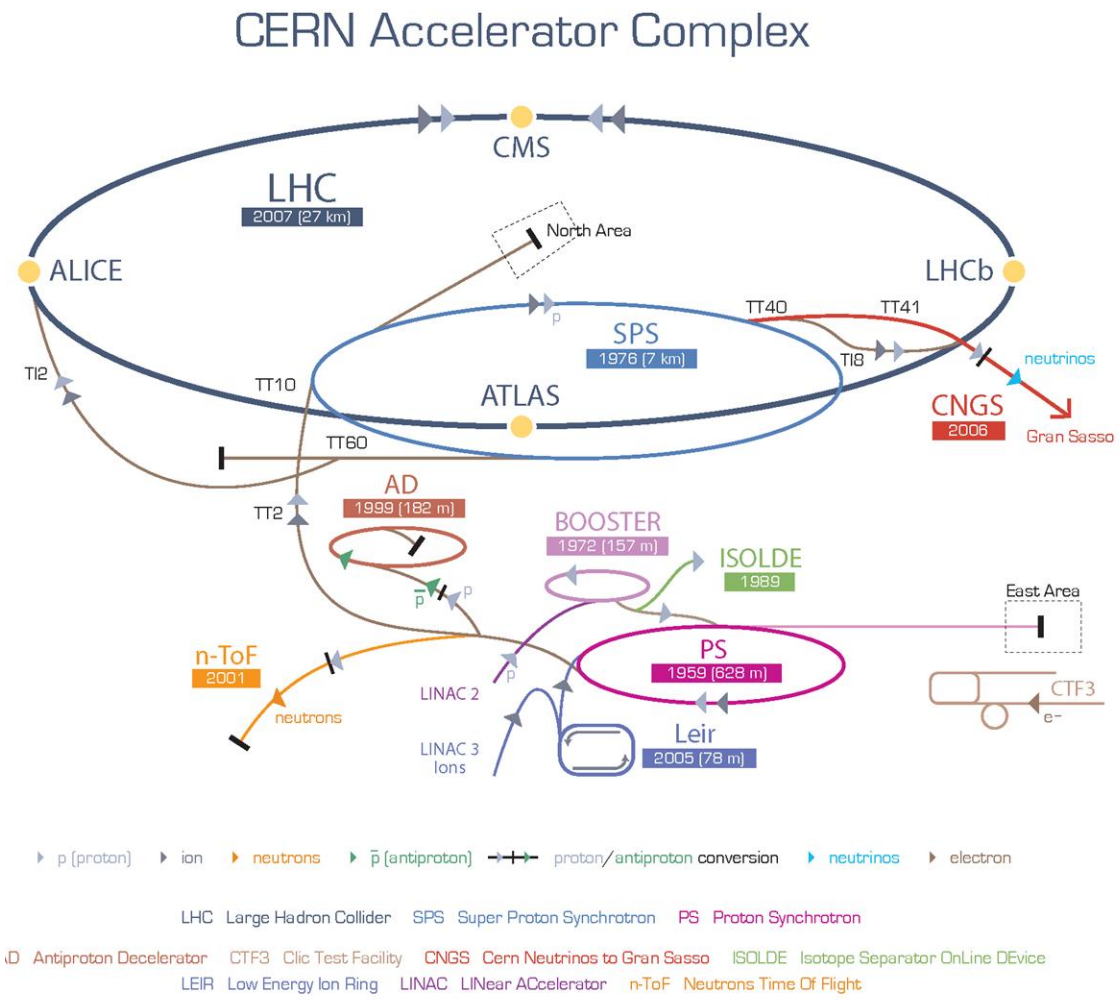

Figure 1.1: Organization of CERN complex

main ring can be seen in figure 1.2. The rings crosses in different points in order to collide the protons and they are divided in eight straight sections and eight arcs. In each octant bunches are controlled by dipole magnets. These magnets, in figure 1.3, need to produce a very strong magnetic field in order to be able to bend a 7 TeV beam of protons. This intense magnetic field, 8.33 T, is produced by electrical currents that are only achievable by means of superconductivity. All the 1232 dipoles operate at a temperature of 1.9 K, under cooling by liquid helium. They also operate under ultra-high-vacuum. The beam lines with a pressure less than 10^{-9} mbar and the whole dipole system with 10^{-6} mbar, that serves also as insulating system from the surroundings. In addition, the LHC main ring has other magnets that focus and correct different characteristics of the beam: 520 quadrupoles, 2464 sextupoles, 1232 octupoles.

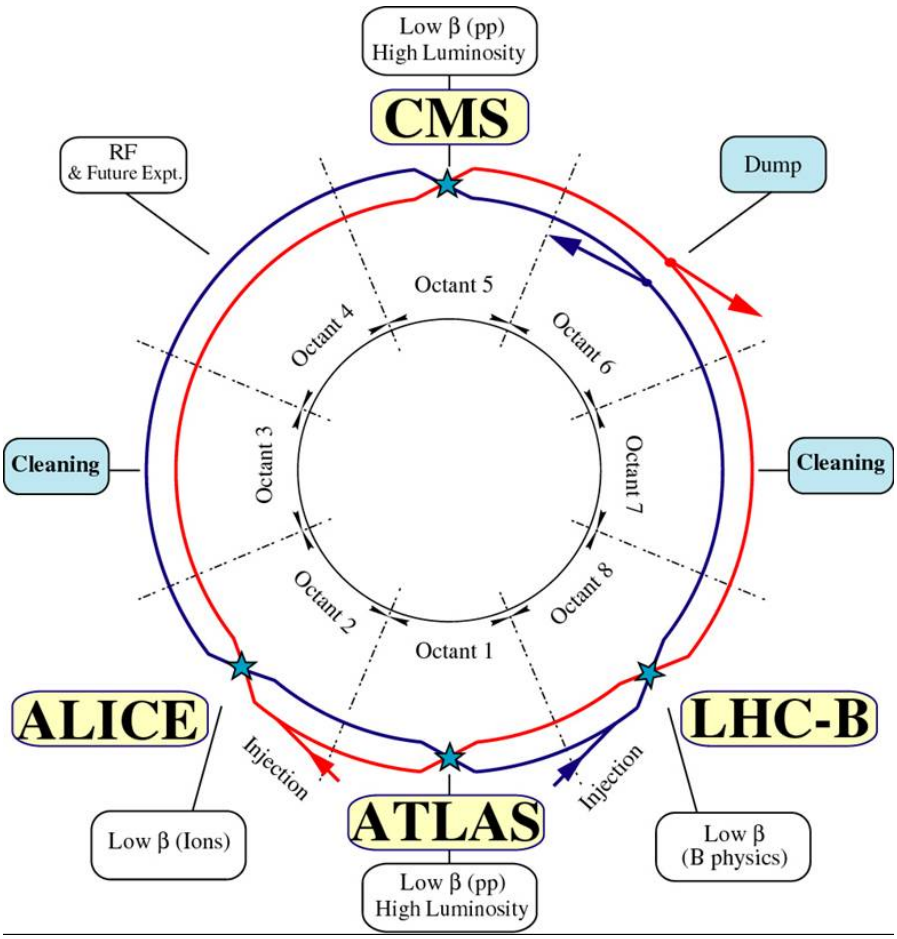

Figure 1.2: Schematic of the LHC main ring design.

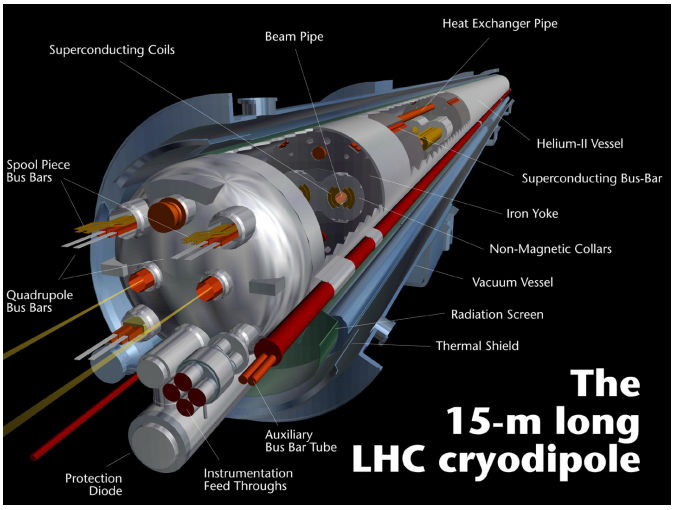

Figure 1.3: Design of LHC cryodipole that bends the beam in the main ring.

Luminosity

On collider physics, such as the LHC, the figure of merit is the luminosity, given in equation 1.1. The luminosity is proportional to the number of events per second, and in this terms is the quantity to be maximized by the design and operation of the accelerator. In terms of the collider characteristics depend on the number of bunches in the ring k_b, the number of protons per bunch N_b, the revolution frequency f_{rev}, the relativistic gamma factor γ, the normalized rms transverse beam emittance ϵ_n and the beta function at the interaction point β^*. The denominator on 1.1 can also be understood in terms of the horizontal and vertical width of the bunches at the crossing. In table 1.1.2 can be found the LHC beam parameters at injection and collision.

$$L = \frac{k_b N_b^2 f_{rev} \gamma}{4\pi \epsilon_n \beta^*} \tag{1.1}$$

Parameter/units	Injection	Collision
Energy [GeV]	450	7000
Luminosity [$\mathrm{cm}^{-2}\mathrm{s}^{-1}$]		10^{34}
k_b Number of bunches	2808	
Bunch spacing [ns]	24.95	
N_b intensity per bunch [protons/bunch]	1.15×10^{11}	
Beam current [A]	0.58	
ϵ_n normalized rms transverse beam emittance [μm]	3.5	3.75
f_{rev} revolution frequency [kHz]	11.25	

At the crossing points, the number of events coming from collisions and produced via an specific process, is directly proportional to the luminosity provided by the collider, as in equation 1.1.

$$N_{events} = L\sigma_{process} \tag{1.2}$$

where $\sigma_{process}$ is the cross section of the process.

The total cross section of a proton-proton collision from the crossing of two bunches at 14 TeV is 100-110 mb [7], from three different scattering processes: elastic, diffractive and inelastic. In the elastic scattering the protons only exchange momenta but their structure remain unchanged, that is the case for the majority of collisions. In diffractive scattering momenta is exchanged and also new particles are produced in addition to the two final protons. Finally, in inelastic scattering, the constituents of the protons, the partons, interchange a big amount of momentum and produce a large quantity of particles. The inelastic processes contribute less than diffraction to the total cross section. While inelastic collisions produce particles in the central rapidity (defined on 1.2.1) region, diffractive and elastic final products have a large rapidity. Only in the hard interactions, inelastic scattering, color is exchanged, being such the reason to fill up the central rapidity region.

From the crossing of two bunches not only one proton-proton interaction is expected. Around 25 interactions are expected for each crossing. Form them, only one is coming from an inelastic collision, that is the type of process of more interest for detectors as CMS or ATLAS. This fact puts an additional difficulty to the detectors in order to extract the hard interaction from all the elastic and diffractive collisions happening at same time. Such phenomena is known as Pile-Up, an illustration of a collision with high pile-up can be found on figure 1.4 as seen by CMS detector.

1.1.3 Run 1

On February 10 of 2013 the first stable run of the LHC reached an end. This run, now called Run 1, started on November 20 of 2009. The original LHC start was planned for 2008, an incident on one of the electric connections of one of the magnets forced to stop the 19th of September of the same year. From the restart on 2009, the energy was augmented from 450 GeV to 4 TeV per beam. The 23th of September 2009 the first collisions were detected by the experiments. One week after the achieved center of mass energy was $\sqrt{s} = 2.36$ TeV, already more than Tevatron (1.98 TeV).

On 2010, from 30th March to 6th December 3.5 TeV per beam were reached delivering near 50 pb^{-1}. With the same energy, approximately 6 fb^{-1} were delivered on 2011.

On 2012, the center of mass energy reached one additional TeV, $\sqrt{s} = 8$ TeV, and around 20 fb^{-1} of integrated luminosity were delivered between April and December. On figure 1.5 can be seen the progress of the recorded luminosity by CMS for 2010-2012 period. The first six weeks of 2013 were devoted to proton-lead collisions.

After this very successful run, the LHC has been stopped for a year for repair and maintenance of different systems in the experiments and in the LHC itself. After this

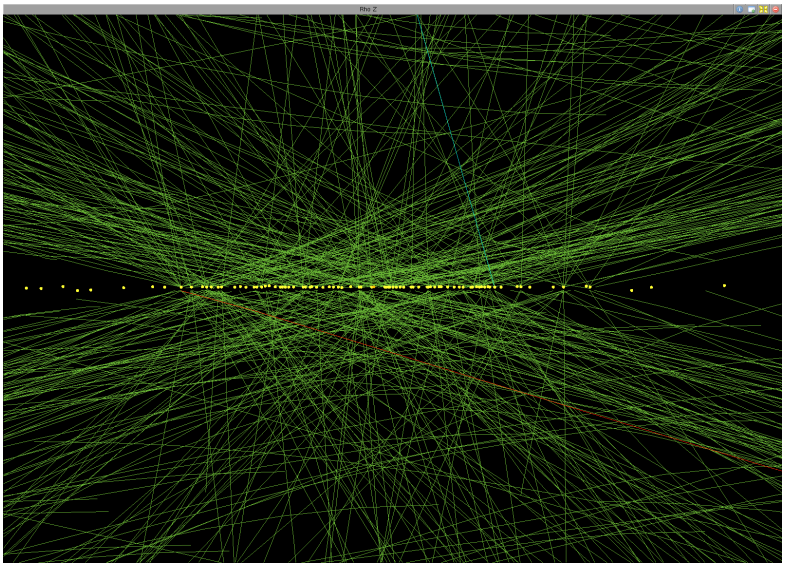

Figure 1.4: High pile-up event (78 interactions) seen by CMS detector. Image credit: Andre Holzner ©CERN

period, known as Long Shutdown or LS1, the LHC is planned to restart a new run on the early spring of 2015.

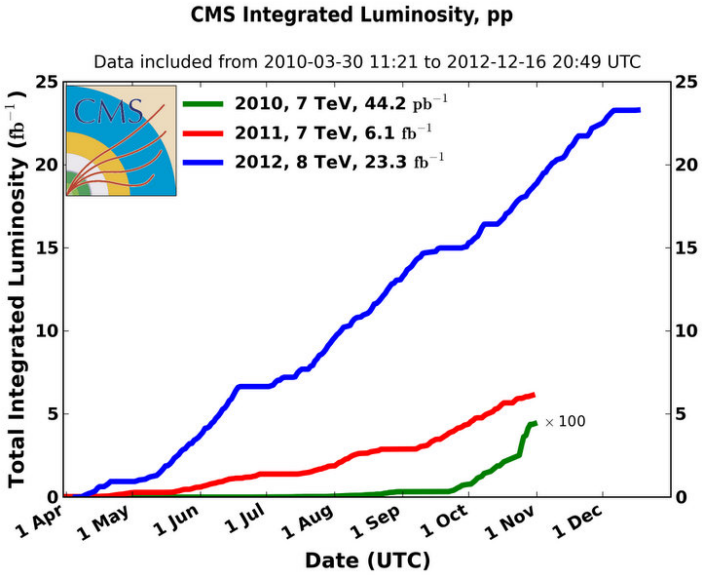

Figure 1.5: CMS integrated luminosity for proton-proton collisions delivered by LHC. ©CERN

1.1.4 Other experiments at LHC

On the main ring there are several experiments depending on the collisions delivered by the LHC main ring. The biggest are CMS [2] and ATLAS [4], both of them generalist experiments designed to do precision measurements as well as new physics searches. Mainly recording proton-proton collisions, they have also recorded ion-ion and proton-ion collisions during the run 1. Both of them were designed for high instantaneous luminosity, $L = 10^{34}\text{cm}^2\text{s}^{-1}$.

In addition, there is other two experiments designed for specific purposes. The LHCb [5] that focus on the study of the physics of the b-hadrons, specially related to the CP violation, and ALICE [6] build for the study of strongly interacting matter. The first of them record proton-proton collisions at an instantaneous luminosity of $10^{32}\text{cm}^2\text{s}^{-1}$ and the second record ion-ion collision with $L = 10^{27}\text{cm}^2\text{s}^{-1}$.

The CMS experiment is going to be described in detail on section 1.2. On the following sections we are going to present very briefly the other three experiences mentioned above.

ATLAS

The ATLAS experiment (A Toroidal LHC ApparatuS) is the biggest LHC experiment. It's located at point one, as displayed on figure 1.2, on the LHC main ring. It's cylindrical detector similar to CMS. It's about 45 meter long, 25 meter high, and weights around 7000 tons. ATLAS main components are, from inside to outside, a tracking system, an electromagnetic calorimeter, an hadron calorimeter and muon chambers. In between this subsystems there is an internal solenoidal magnet and a set of external toroidal magnets. The detector design is presented on figure 1.6.

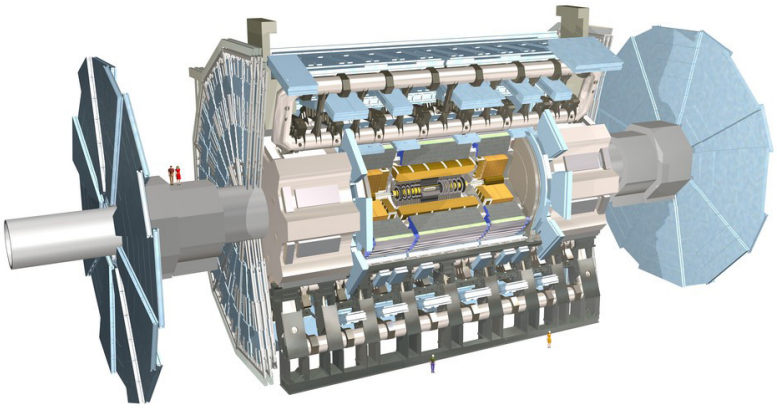

Figure 1.6: ATLAS detector internal view. ©CERN

On the human resources side, ATLAS experiment configures a collaboration of around 3000 persons, coming from 117 universities around the world, from 38 countries. A third part of the collaboration are students.

LHCb

LHCb detector, hosted at point 8 of the LHC main ring, has a different design than CMS and ATLAS. Smaller than these, it's design mainly focus to be able to detect particles produced close to the beam direction. Reason why is not cylindrically but conically shaped. It also has the same main parts, a tracking system with a very precise vertex locator, electromagnetic and hadron calorimeters, muon chambers and magnets. It's major specificity is a system that allows to distinguish different hadrons, what is crucial for the study of strong interacting matter. It measures 21 m long, 10 m high and 13 m wide, and weights 4500 tons. A view of the detector can be found on figure 1.7. The LHCb collaboration groups around 700 persons from 50 different universities over 15 countries.

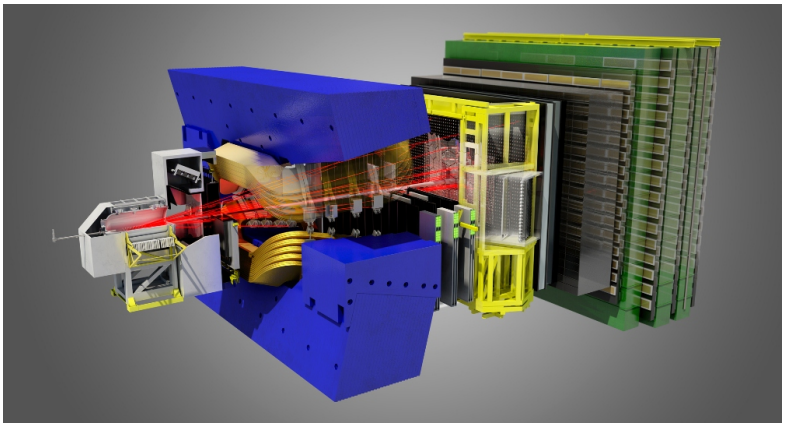

Figure 1.7: LHCb detector internal view. ©CERN

ALICE

The ALICE experiment (A Large Ion Collider Experiment) is located at point 2 of the LHC main ring, measures 16 m high, 16 m wide and 26 m long, and weights 10000 tons. It's an asymmetrical detector as LHCb. It's structure can be seen on figure 1.8. ALICE collaboration counts around 1500 people, from 154 physics institutes in 37 countries.

1.2 The Compact Muon Solenoid experiment

The CMS detector, hosted at point 5 of the LHC main ring (see figure 1.2), is the second biggest LHC experiment. Cylindrically shaped, measures 15 m of diameter and 28.7 m long, but weights 14000 making it the heaviest LHC experiment. Its subsystems are concentrically located from the collision point in the beam line. It's main characteristic is the strong 3.8 T solenoid magnet. A representation of the detector can be found in

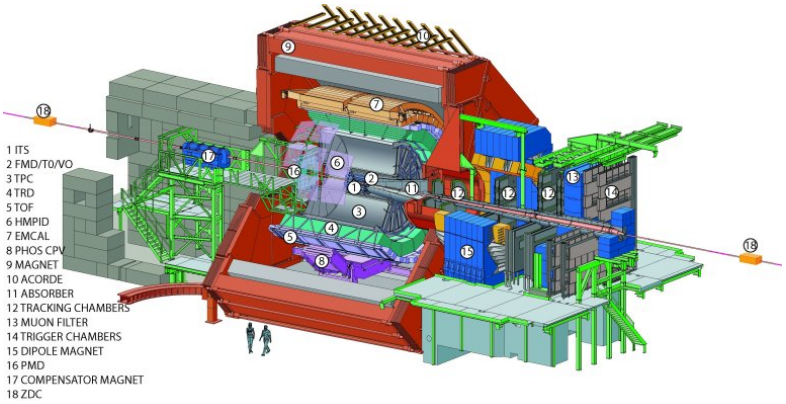

Figure 1.8: ALICE detector internal view. ©CERN

figure 1.9. The CMS collaboration is formed by around 2600 scientists, of which 900 are students, from 181 institutes over 41 countries.

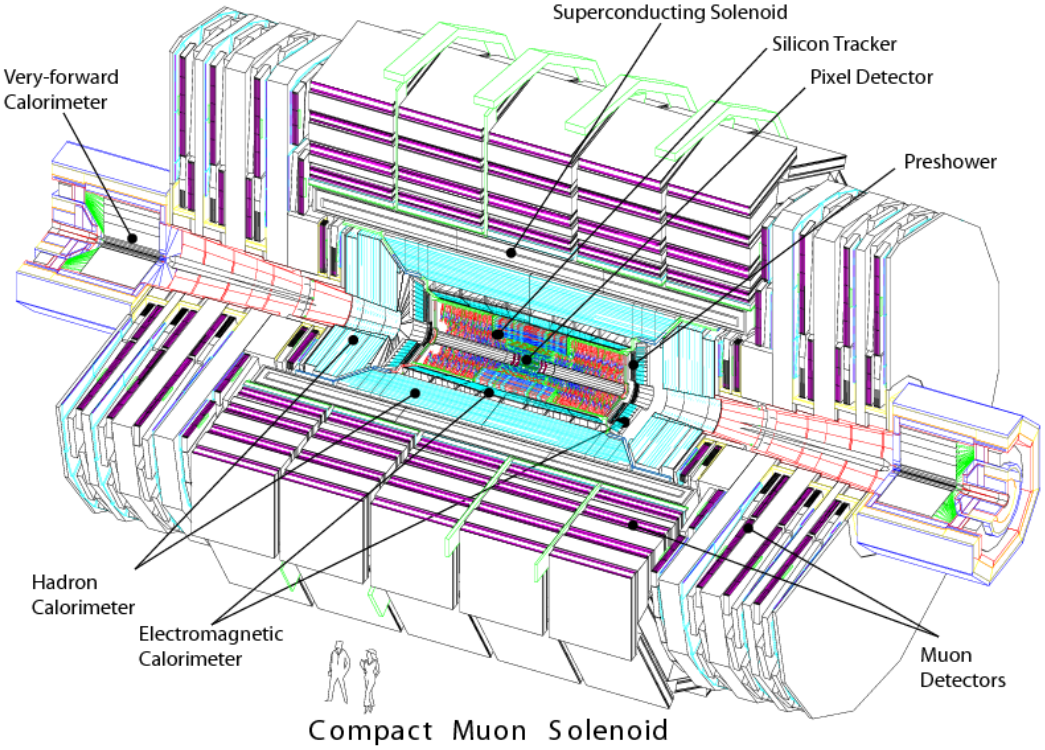

Figure 1.9: CMS detector internal view. ©CERN

CMS has been designed to be able to do very precise identification of particles originated from the collisions and their properties. For the measurement of the momentum of the charged particles, CMS counts with a very strong magnet that allows to bend very energetic particles. In addition, the calorimeters allow to measure accurately the energy from hadrons, electrons and photons. At the most external layer, the muons chambers measuring muons properties, and in the innermost the tracking system that reconstructs the collision points and the charged particles tracks. In figure 1.10 can be found a representation of the different subsystems of CMS and how particles are reconstructed from them.

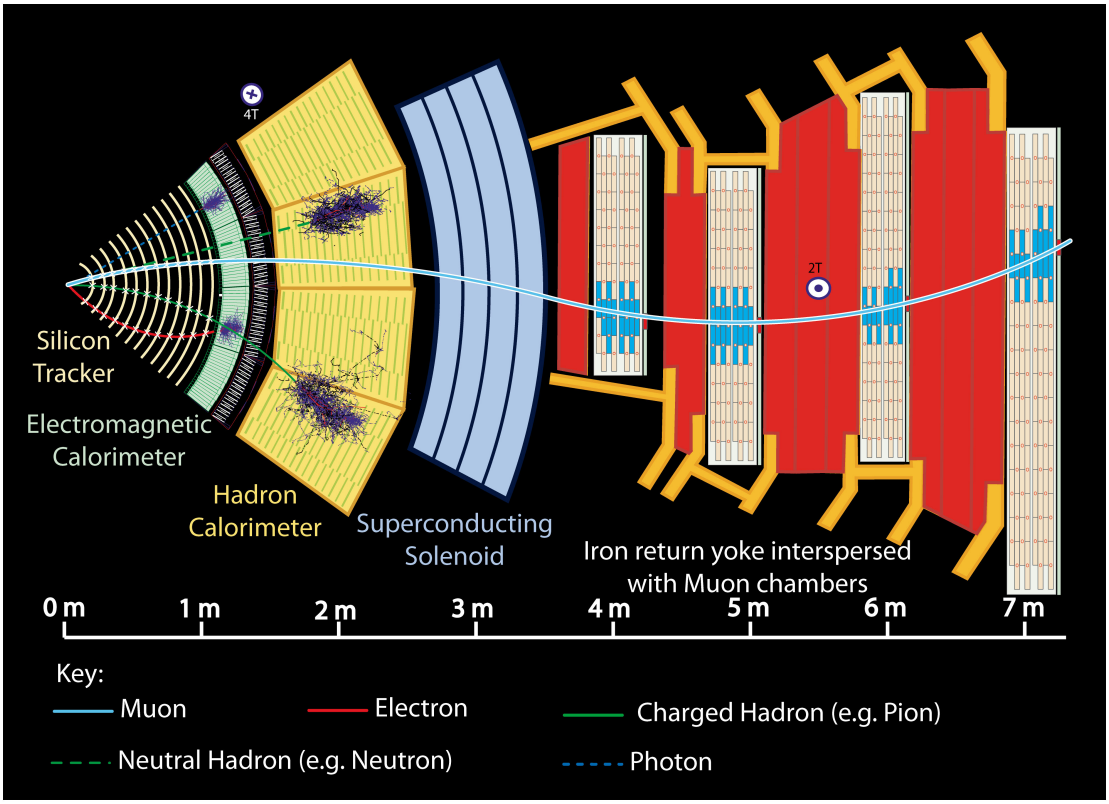

Figure 1.10: CMS sub-detectors and particle identification. ©CERN

1.2.1 Coordinate system

The origin of coordinates defined on the CMS detector is located on the nominal collision point, the "interaction point". From there, the z-axis is defined along the beam pipe line pointing towards the Jura mountains. The positive/negative z-axis directions define the positive/negative sides of the detector. The y-axis is defined towards the zenith and the x-axis towards the center of the LHC ring. Due to the inclination of the LHC plane, this

coordinate system is slightly tilted with respect to the true vertical. A representation of the coordinate system definition can be found in figure 1.11.

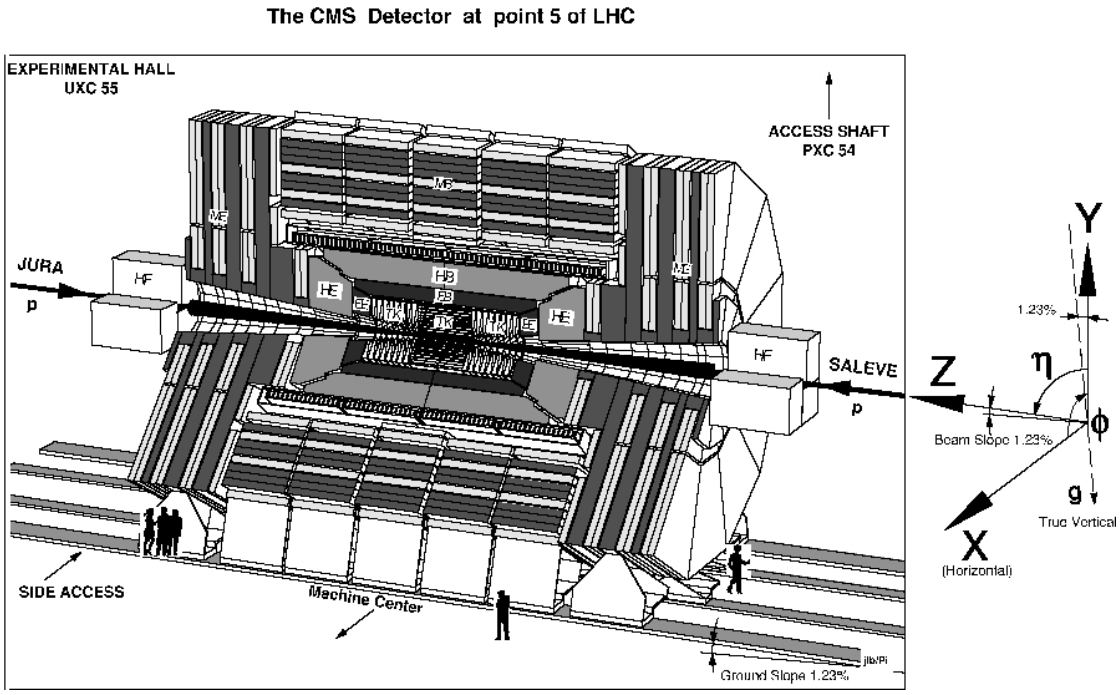

Figure 1.11: CMS coordinate system. ©CERN

We can also define two the ϕ angle in the x-y plane from the x-axis towards the positive y-axis, and the θ angle in the z-y plane from z-axis towards the positive y-axis. In experimental particle physics is preferred to work with relativistic invariant quantities, reason why instead of working with θ we define the pseudorapidity η, equation 1.3.

$$\eta = -\ln\left(\tan\left(\frac{\theta}{2}\right)\right) \tag{1.3}$$

One can define another relativistic invariant quantity, the rapidity y as from equation 1.4. With $\boldsymbol{p}$ being the momentum vector and E the energy of a given particle, p_L denotes its longitudinal component, that in our case is the same z-component.

$$y = \frac{1}{2}\ln\left(\frac{E + p_L}{E - p_L}\right) \tag{1.4}$$

On the limit that the mass of the particle is very small compared to its momentum, one can replace approximate the particle energy by the momentum magnitude, giving rise to the definition of the pseudorapidity in terms of the momentum of the particle $\eta = \frac{1}{2}\ln\left(\frac{\boldsymbol{p}+p_L}{\boldsymbol{p}-p_L}\right)$

We define also the radial coordinate over the x-y plane, plane that is called the transverse plane being orthogonal to the longitudinal direction, the z-axis. In such plane are also defined the transverse quantities of particles, as the transverse momentum p_T. Finally, for any two objects an angular distance can be defined in the $\eta - \phi$ plane, as in equation 1.5.

$$\Delta R = \sqrt{(\Delta\eta)^2 + (\Delta\phi)^2} \tag{1.5}$$

1.2.2 Magnet

In order to measure the momentum of the charged particles going inside the detector is crucial to apply the correct magnet field, sufficiently strong to bend very energetic particles. The momentum of a charged particle inside an uniform magnetic field can be written as

$$p = \gamma m v = qBr \tag{1.6}$$

where B is the magnitude of the magnetic field, γ the usual relativistic factor, m the mass of the particle, v its rapidity, q its charge and r the bending radius. The sagitta of the arc is

$$s = \frac{L^2}{8r} = \frac{qBL^2}{8p} \tag{1.7}$$

with L the distance the particle moved inside the magnetic filed. Inside a solenoid L is equal to the radius of it.

From relation 1.7 is possible to deduce that the resolution on the momentum of the particle has an inverse dependence with the magnetic field and the radius of the solenoid, as shown in equation 1.8. From there, for a better resolution is needed to increase the magnetic field and the radius of the solenoid.

$$\frac{dp}{p} \propto \frac{p}{BL^2} \tag{1.8}$$

The design of CMS magnet target both features, it utilizes a large solenoid of 6 m of diameter and 13 m long. It's made of 4 layers of windings of NbTi cable that is cooled to 4.45 K in order to achieve the superconducting state. This magnet is able to produce an uniform magnetic field inside it of 3.8 T. Outside the magnet 5 wheels and 3 disks of iron are placed in order to return the flux of the magnetic field, inducing just a 2 T radial magnetic field outside the solenoid. This iron yoke contributes with most of the weight of the detector, 10000 tons. In between the iron yoke the muon chambers are placed.

1.2.3 Tracker system

1.2.4 Electromagnetic calorimeter

1.2.5 Hadronic Calorimeter

1.2.6 Muon chambers

1.2.7 Trigger

Chapter 2

The Standard Model

Since the Greeks, different theories about the composition and structure of the world have been formulated. At ancient Greece this theories were elaborated from a philosophical point of view. Nowadays, we count with a very sophisticated set of tools and concepts that allowed us to build up a general vision of nature, its components and structure. Moreover, on the subject of the constituents, or elemental constituents, we have developed a theory that is capable to describe the majority of known phenomena. This theory is the Standard Model (SM) of particle physics.

This SM relies in two of the more fancy constructs of modern physics and mathematics. From physics side, the quantum field theory; from mathematics, group theory. Quantum field theory has born from the understanding of processes that take place at very small spatial scales but in a regime where special relativity play an important role. To describe such, a major part of the most brilliant minds of the 20th century dedicated their life, Paul Dirac, Richard Feynman, Enrico Fermi among them. The theory of quantum fields has set in a common place two extraordinary achievements of physics: special relativity and quantum mechanics. With it we have been capable to describe many phenomena: β decay and α decay, solid state, with many other.

From the mathematics side, group theory has become one of the most powerful tools for particle physicist. However, their development began quite early, with Galois at XXXX, and was used in other parts of physics, it's with Lie algebras and the possibility of describing continuous symmetries that the most important step will be given. Also, this would have not been possible with the amazing connection found by Emmy Noether in XXXX. Her finding connected symmetries and physics in a form never known before. She found that for every conserved quantity in a system there is a symmetry followed by it. As group theory can be seen, in grosso modo, a way to mathematically describe symmetries, group theory became the tool to describe systems with conserved quantities.

In this chapter, we are going to present the basics of the SM. We describe its seminal ideas, it structure and content and it's ultimate consequences. Finally, we close with its limitations.

2.1 Symmetires and interactions

2.2 Fields and particles

2.2.1 The mass problem

2.2.2 Spontaneous Symmetry Breaking

2.2.3 Higgs mechanism

2.3 Hierarchy problem and other limitations

Chapter 3

Vector Like Quarks: Generic model

From chapter 2 we have seen how there are some parts in the SM that does not work very well. From such internal issues some further models/theories have been developed. All this theories are commonly grouped under the term Beyond Standard Model or simply BSM. One of the most famous BSM theory is supersymmetry (SUSY). This theory postulates a symmetry that does not distinguish between fermions and bosons. This idea have given birth to a plethora of model realizations and physics predictions. So far, nothing of the new consequences of this theory have been confirmed but the experiments have an enormous investment on their search. But not only SUSY have seen the day light, there is on the market an astonishing amount of BSM theories addressing different issues of the SM. Extra dimensions, fourth families, composite Higgs are a few of them.

In this chapter we will describe a bunch of models that introduce additional heavy quarks, heavier than the top, in order to solve the hierarchy problem, described on section 2.3.

3.1 Motivation

3.2 Generic Formulation

3.3 Fesability study for a search of a T at LHC at 8 TeV

3.3.1 Production modes

3.3.2 Decay modes

3.3.3 Stragey for the full hadronic final state

3.3.4 Event selection

3.3.5 Results

Chapter 4

Understanding theory predictions via Monte-Carlo event generation

However we have nowadays a very elegant and complete theoretical description of particle physics, is not always evident how to translate this theory in actual predictions, in actual measurements. Moreover, on the case of hadronic colliders, as the LHC, it's even more difficult due to the particularities of strong interaction. On this subject, a set of tools and approaches have been developed in order to be able to make accurate predictions from theory that could be directly researched for on the experiments, as CMS or ATLAS for example. In the present chapter, we describe such tools and formalisms and a set of studies comparing the well behavior of this tools with data.

4.1 Mote-Carlo formalism

4.1.1 Partonic step

4.1.2 Hadronic step

4.1.3 Detector step

4.2 Tools

4.2.1 Matrix-element generators

4.2.2 Hadron generators

4.2.3 Detector simulation

4.3 Validation on data

Chapter 5

Search for a single produced T' decaying into top and Higgs in the full hadronic final state

In the present chapter we describe in full detail the search performed using 2012 data collected by CMS for a T' in the full hadronic final state. The theoretical formalism for such object has been described on chapter 3.

5.1 Analysis Strategy

5.2 Datasets

5.3 Event selection

5.3.1 T' reconstruction with a χ^2 sorting algorithm

5.3.2 Efficiencies

Trigger

Selection

5.4 Background estimation from data

5.4.1 Known difficulties and tried methods

5.4.2 Method

5.4.3 Validation

5.5 Systematics

5.6 Results

Bibliography

[1] O. S. Brüning, P. Collier, P. Lebrun, S. Myers, R. Ostojic, J. Poole, and P. Proudlock, *LHC Design Report*. CERN, Geneva, 2004.

[2] **CMS Collaboration** Collaboration, G. L. Bayatian *et al.*, *CMS Physics: Technical Design Report Volume 1: Detector Performance and Software*. Technical Design Report CMS. CERN, Geneva, 2006. There is an error on cover due to a technical problem for some items.

[3] **CMS Collaboration** Collaboration, G. L. Bayatian *et al.*, "CMS Physics: Technical Design Report Volume 2: Physics Performance," *J. Phys. G* **34** no. CERN-LHCC-2006-021. CMS-TDR-8-2, (2007) 995–1579. 669 p. revised version submitted on 2006-09-22 17:44:47.

[4] **ATLAS Collaboration** Collaboration, A. Collaboration, *ATLAS detector and physics performance: Technical Design Report*. Technical Design Report ATLAS. CERN, Geneva, 1999. Electronic version not available.

[5] **LHCb Collaboration** Collaboration, J. Alves, A. Augusto *et al.*, "The LHCb Detector at the LHC," *JINST* **3** (2008) S08005.

[6] **ALICE Collaboration** Collaboration, P. Cortese, C. W. Fabjan, L. Riccati, K. Safarík, and H. de Groot, *ALICE physics performance: Technical Design Report*. Technical Design Report ALICE. CERN, Geneva, 2005. revised version submitted on 2006-05-29 15:15:40.

[7] **UA4/2 Collaboration** Collaboration, C. Augier *et al.*, "Predictions on the total cross-section and real part at LHC and SSC," *Phys.Lett.* **B315** (1993) 503–506.

Contents